

# Thermodynamic comparison of PNA/DNA and DNA/DNA hybridization reactions at ambient temperature

Frederick P. Schwarz\*, Scott Robinson and John M. Butler<sup>1</sup>

Center for Advanced Research in Biotechnology/National Institute of Standards and Technology, 9600 Gudelsky Drive, Rockville, MD 20850, USA and <sup>1</sup>Biotechnology Division, National Institute of Standards and Technology, Gaithersburg, MD 20899, USA

Received July 28, 1999; Revised and Accepted October 26, 1999

## ABSTRACT

The thermodynamics of 13 hybridization reactions between 10 base DNA sequences of design 5'-ATGCXYATGC-3' with X, Y = A, C, G, T and their complementary PNA and DNA sequences were determined from isothermal titration calorimetry (ITC) measurements at ambient temperature. For the PNA/DNA hybridization reactions, the binding constants range from  $1.8 \times 10^6 \text{ M}^{-1}$  for PNA(TT)/DNA to  $4.15 \times 10^7 \text{ M}^{-1}$  for PNA(GA)/DNA and the binding enthalpies range from  $-194 \text{ kJ mol}^{-1}$  for PNA(CG)/DNA to  $-77 \text{ kJ mol}^{-1}$  for PNA(GT)/DNA. For the corresponding DNA/DNA binding reactions, the binding constants range from  $2.9 \times 10^5 \text{ M}^{-1}$  for DNA(GT)/DNA to  $1.9 \times 10^7 \text{ M}^{-1}$  for DNA(CC)/DNA and the binding enthalpies range from  $-223 \text{ kJ mol}^{-1}$  for DNA(CG)/DNA to  $-124 \text{ kJ mol}^{-1}$  for DNA(TT)/DNA. Most of the PNA sequences exhibited tighter binding affinities than their corresponding DNA sequences resulting from smaller entropy changes in the PNA/DNA hybridization reactions. van't Hoff enthalpies and extrapolated  $\Delta G$  values determined from UV melting studies on the duplexes exhibited closer agreement with the ITC binding enthalpies and  $\Delta G$  values for the DNA/DNA duplexes than for the PNA/DNA duplexes.

## INTRODUCTION

Peptide nucleic acids (PNAs) are DNA analogs where the four nucleotides, adenine (A), thymine (T), guanine (G), and cytosine (C), are attached to a *N*-(2-aminoethyl)glycine backbone instead of the negatively charged deoxyribose phosphate backbone in DNA (1–4). Since the spacing between the nucleotides is the same as in DNA, the conventional Watson–Crick base pairing rules apply between mixed base PNA/DNA sequences resulting in the formation of B-like helical duplexes (5). UV monitored melting (UVM) studies of PNA hybrid duplexes in solution have shown that the PNA sequences can bind to their complementary single-strand DNA (5), RNA (6), and PNA (7) sequences with greater affinities than do their corresponding DNA sequences. In addition, UVM studies of these duplexes show that a single base mismatch in a PNA/DNA duplex is less

stable than the same mismatch in the corresponding DNA/DNA duplex (5). The higher affinity and specificity of PNA sequences binding to their complementary DNA sequences have resulted in applications in DNA mutation detection (8,9) affinity capture (10,11), PCR clamping (12,13), and inhibition of enzymatic activity (14–16). PNAs have also been used as effective sequence-specific, solid-phase DNA hybridization biosensors (17).

A significant amount of PNA research has been focused on the characterization of PNA interactions with other nucleic acids using UVM (5–7), linear and circular dichroism (18), NMR spectroscopy (6,19), X-ray crystallography (20–22), and mass spectrometry (23–25). Despite much research in characterizing PNA/DNA interactions, the only thermodynamic data on PNA/DNA hybridization interactions have been determined indirectly from UVM studies of the resulting PNA/DNA duplexes (2). Thermodynamic data on PNA/DNA binding interactions are not only important in understanding PNA/DNA interactions but also are necessary for the development of thermodynamic models for the design of PNA sequences with specific DNA hybridization properties. For example, the computer software used today in the design of PCR primers utilizes thermodynamic data collected from DNA/DNA interactions (26). It has been shown that the thermodynamics of a DNA/DNA binding reaction is dependent on its base sequence, particularly the nearest neighbor Watson–Crick pairs (27), and, thus, the thermodynamics of a PNA/DNA hybridization reaction may also be predictable from its sequence. Improvements in this predictive scheme have recently been reported by Santa Lucia *et al.* (28). Because the structure of the PNA backbone is uniquely different from DNA, using thermodynamic models based upon DNA thermodynamic data will most likely not be accurate in designing PNA probes. In fact, Giesen *et al.* (29) found that to predict the melting temperature of PNA/DNA duplexes from the nearest neighbor interactions, as is done for DNA/DNA duplexes, additional factors of length and the pyrimidine content of the duplex had to be included. To develop a thermodynamic predictive model, it is first necessary to develop a library of thermodynamic data on PNA/DNA hybridization reactions in terms of the binding constant ( $K_b$ ), the binding enthalpy ( $\Delta H_b^\circ$ ), the binding entropy ( $\Delta S_b^\circ$ ), and the Gibbs energy change ( $\Delta G_b^\circ$ ). Since there is some evidence that the final dissociative state of the PNA at temperatures above 313 K is not the same as at ambient temperature (30,31), it is intrinsically more accurate to determine these quantities

\*To whom correspondence should be addressed. Tel: +1 301 738 6219; Fax: +1 301 738 6255; Email: fred@carb.nist.gov



experimental mass per mole, the calculated mass per mole, and the difference in terms of mass % are presented in Table 1. Although the PNA(CC) sequence is only 85.6 mol % pure, its thermodynamic binding quantities are included only for comparison to the other sequence values. The buffer (PBS buffer) was made up to 10 mM sodium phosphate concentration using appropriate masses of sodium diphosphate and sodium monophosphate to maintain a pH of 7.0 and contained 0.1 M sodium chloride and 0.1 mM sodium EDTA. Known milligram quantities of the DNA and PNA oligomers, using a Mettler AE163 electrobalance accurate to 0.01 mg, were dissolved directly into known volumes of the buffer and the concentrations of the DNA and PNA strands in solution were determined by UV absorption measurements at 260 nm. For the DNA sequences, an enzymatic method consisting of exhaustive hydrolysis of the sequences with snake venom phosphodiesterase was employed to determine the extinction coefficient for each sequence (33). This method consisted of dissolving the lyophilized DNA sequence in 200  $\mu$ l of 0.2 M Tris-HCl buffer containing 15 mM MgCl<sub>2</sub> at pH 9.0, measuring its optical density, adding 0.05 U of *Crotalus durissus terrificus* phosphodiesterase (CAS registry no. 9025-82-5) from Boehringer Mannheim to the sample and reference solutions, heating the sample to 310 K for 1 h to ensure complete hydrolysis, and then re-measuring the optical density of the sample. The substrate thymidine 5'-monophosphate *p*-nitrophenyl ester (CAS registry no. 98179-10-3) from Sigma Chemical Co. was added to the samples and the appearance of a yellow color due to hydrolysis of the substrate by the enzyme showed that the enzyme was still active. The concentration of the sequence was then calculated using an extinction coefficient obtained by adding the extinction coefficients 15.4, 7.4, 11.5, and  $8.7 \times 10^3$  M<sup>-1</sup> cm<sup>-1</sup> for, respectively, the A, C, G, and T bases in the sequence. This concentration was then used to determine the extinction coefficient of the original sequence from its optical density prior to hydrolysis. With the exception of DNA'(TT), DNA'(GG), DNA'(TC), DNA(AG), DNA(CC), and DNA(CT), the extinction coefficients were within the experimental error (3%) of the calculated extinction coefficients determined by the nearest-neighbor method (34). The extinction coefficients employed in determination of the DNA sequences are presented in Table 2. For the PNA sequences, the extinction coefficient was  $1.0 \times 10^5$  l mol<sup>-1</sup> cm<sup>-1</sup> for all the PNAs except PNA(TA) and PNA(TG), where the extinction

coefficient was  $1.1 \times 10^5$  l mol<sup>-1</sup> cm<sup>-1</sup>, as recommended by the supplier. The extinction coefficients for PNA(GA), PNA(CT), PNA(AA), and PNA(AG) were assumed to be  $1.0 \times 10^5$  l mol<sup>-1</sup> cm<sup>-1</sup> since they were not available from the supplier. Attempts to determine the extinction coefficients for the PNA sequences using exhaustive hydrolysis by phosphodiesterase were unsuccessful since the enzyme failed to hydrolyze the PNA sequences.

### ITC measurements

All calorimetric titrations were performed according to the methods of Wiseman *et al.* (35) and Schwarz *et al.* (36) using a Microcal Omega titration calorimeter. The Omega titration calorimeter consists of a matched pair of sample and reference vessels (1.374 ml) containing the PNA or DNA in phosphate buffer and the buffer solution, respectively. Five to ten microliter aliquots of the complementary DNA solution at concentrations 10–20 $\times$  the oligomer concentration in the sample vessel were added 3–4 min apart to the sample solution ranging in concentration from 0.01 to 0.1 mM. The titrations were continued for several additions past saturation so that a heat of dilution of the titrant could be determined from these additional peak areas. Some of the heats of dilution, particularly the large values, were checked by titrating the titrant directly into the buffer and were found to be the same. The heats of dilution were then subtracted from the heats obtained upon titrating the complementary DNA solution into the oligomer solution in the sample vessel.

A non-linear, least squares minimization software program (Origin 2.9 from Microcal Inc.) was used to fit the incremental heat of the *i*th titration [ $\Delta Q(i)$ ] of the total heat,  $Q_t$ , to the total complementary DNA titrant concentration,  $X_t$ , according to the following equations,

$$Q_t = nC_t \Delta H_b^\circ V \{1 + X_t/nC_t + 1/nK_b C_t - [(1 + X_t/nC_t + 1/nK_b C_t)^2 - 4X_t/nC_t]^{1/2}\} / 2 \quad 2a$$

$$\Delta Q(i) = Q(i) + dV_i/2V \{Q(i) + Q(i-1)\} - Q(i-1) \quad 2b$$

where  $C_t$  is the total PNA or DNA strand concentration in the sample vessel,  $V$  is the volume of the sample vessel, and  $n$  is the stoichiometry of the binding reaction, which should be 1.0 but was allowed to vary to further verify the determination of the DNA and PNA concentrations. The accuracy of the DNA concentrations was, indeed, verified by the observed

**Table 2.** Extinction coefficients of the DNA sequences at 260 nm

Extinction coefficient ( $\times 10^5$ l mol <sup>-1</sup> cm <sup>-1</sup> )	DNA sequence (5'→3')		
9.1	DNA(CC) = ATGCCCATGC	DNA'(CC) = GCATCCGCAT	
9.2	DNA(TC) = ATGCTCATGC	DNA'(TC) = GCATTCGCAT	DNA'(CT) = GCATCTGCAT
9.3	DNA(GA) = ATGCCCATGC	DNA(CT) = ATGCCATATGC	DNA'(TT) = GCATTTGCAT
9.4	DNA(TT) = ATGCTTATGC	DNA'(CG) = GCATCGGCAT	
9.5	DNA(TG) = ATGCTGATGC	DNA'(TG) = GCATTGGCAT	DNA'(GT) = GCATGTGCAT
9.5	DNA(CG) = ATGCCGATGC		
9.6	DNA(AC) = ATGCACATGC	DNA(CA) = ATGCCAATGC	
9.7	DNA'(CA) = GCATCAGCAT	DNA'(AC) = GCATACGCAT	DNA'(GG) = GCATGGGCAT
9.7	DNA(GG) = ATGCGGATGC	DNA(GT) = ATGCGTATGC	DNA(TA) = ATGCTAATGC
9.8	DNA'(TA) = GCATTAGCAT		
10.0	DNA(AA) = ATGCAAATGC	DNA(AG) = ATGCAGATGC	DNA'(GA) = GCATGAGCAT
10.0	DNA'(AA) = GCATAAGCAT	DNA'(AG) = GCATAGGCAT	

stoichiometry of  $n = 0.97 \pm 0.06$  in titrations of the DNA titrant against its complementary DNA sequence inside the sample vessel. This same DNA titrant solution was then employed as the titrant in the PNA titrations. For the DNA into PNA titrations, the average stoichiometry was  $0.96 \pm 0.06$  which arises from inaccuracy in the DNA titrant and PNA concentrations. Binding entropies,  $\Delta S_b^\circ$ , were calculated from

$$\Delta S_b^\circ = (\Delta H_b^\circ - \Delta G_b^\circ)/T \quad 3$$

where

$$\Delta G_b^\circ = -RT \ln(K_b) \quad 4$$

and the ideal constant  $R = 8.31451 \text{ J mol}^{-1} \text{ K}^{-1}$ .

The uncertainties in the values of  $K_b$  and  $\Delta H_b^\circ$  determined from several titrations of the DNA titrant into either the complementary DNA or PNA solutions in the sample cell represent only random errors inherent in the ITC measurements. There are also possible systematic errors which are combined in quadrature with these random errors to obtain a combined standard uncertainty for the final reported values of  $K_b$  and  $\Delta H_b^\circ$ . Estimates of these systematic standard uncertainties are  $0.03 K_b$  and  $0.03 \Delta H_b^\circ$  resulting from uncertainty in the solution concentrations,  $0.01 K_b$  and  $0.01 \Delta H_b^\circ$  resulting from uncertainty in the ITC calibration, and  $0.005 K_b$  and  $0.005 \Delta H_b^\circ$  resulting from uncertainty in the titrant and cell volumes.

#### UVM measurements

The duplex products from the ITC measurements were diluted with the buffer to an optical density range of 0.2–0.8 at 260 nm as monitored by a Perkin Elmer Lambda 4B spectrophotometer. The sample cell containing the duplex solution was then heated at a rate of  $1 \text{ K min}^{-1}$  by means of a thermal electric heater while the reference cell containing just the buffer solution was maintained at room temperature. It was observed that the optical density of the buffer in the sample cell remained within an OD error of 0.002 from 288 to 363 K so that any increase in the optical density of the duplex solution at 260 nm resulted from changes in the optical density of the duplex alone. The resulting increase in the optical density of the sample solution was recorded every 30 s over the temperature range 290–363 K and repeated for the transitions with low transition temperatures from 288 to 363 K. The results were analyzed by EXAM (37), a software program which normalized the optical densities to the total optical density change and fitted the normalized data to a two-state transition model. The extent of single strand formation,  $\alpha(T)$ , is, thus, the normalized optical density at temperature  $T$ . The temperature at the midpoint of the transition where  $\alpha(T_m) = 0.5$  is the transition or melting temperature,  $T_m$ , and the van't Hoff enthalpy for the transition,  $\Delta H_v$ , is for dissociation of a duplex into two complementary strands (38)

$$\Delta H_v = 6R(T_m)^2 d\alpha(T_m)/dT \quad 5$$

where  $d\alpha(T_m)/dT$  is the slope of the normalized optical density versus temperature curve at  $T_m$ .

The equilibrium constant for the transition of a duplex into two non-self complementary strands is  $4C_t^{-1}$  at the transition temperature (38).  $C_t$  is the total strand concentration and was determined by dividing the optical density by an extinction coefficient determined as the sum of the DNA and PNA single

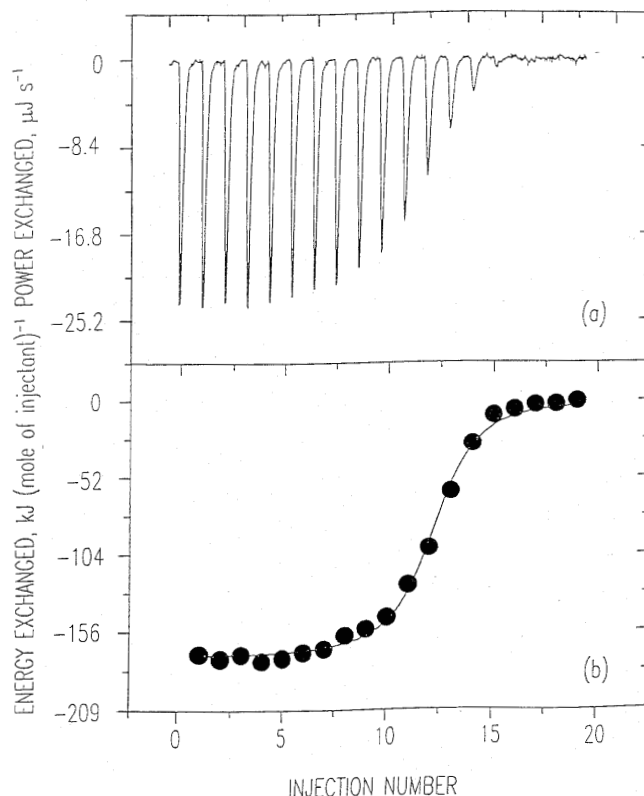


**Figure 1.** (a) The ITC scan consisting of the addition of 5  $\mu\text{l}$  aliquots of 0.801 mM DNA'(CA) to its complementary DNA(TG) sequence (0.037 mM) in PBS buffer at 297.0 K. (b) The binding isotherm for this titration.

strand extinction coefficients divided by 2. Since  $C_t$  is the total strand concentration from the ITC measurements where the titrations were completed just beyond the saturation point, then the duplex concentration is  $\sim C_t/2$ . This concentration was used to determine  $\Delta G_b^\circ$  (UVM) and, thus, an error in the duplex concentration by adding an excess at most of 10% titrant in the ITC measurements would only introduce an error of 5% in  $C_t/2$  and  $0.12 \text{ kJ mol}^{-1}$  in  $\Delta G_b^\circ$  (UVM). The binding affinity at ambient temperature was then calculated using the following form of the van't Hoff equation,

$$\Delta G_b^\circ (\text{UVM}) = -RT \ln\{4C_t^{-1}\} - \Delta H_v(1 - T/T_m) \quad 6$$

The van't Hoff enthalpies that showed the largest discrepancy with the ITC determined binding enthalpies were also determined from the slope of a plot of  $1/T_m$  as a function of  $\ln\{\text{OD}\}$  (39) where the OD ranged from 0.08 to 2.00, the temperature range was from 287 to 363 K, and at least five or six data points were used for the fits. (Although in Borer *et al.* (39)  $1/T_m$  was plotted as a function of  $\ln\{C_t\}$ ,  $\ln\{\text{OD}\}$  is used here since  $C_t = \{\text{OD}\}/[0.5 \epsilon(\text{DNA}) + 0.5 \epsilon(\text{PNA})]$  and  $0.5 \epsilon(\text{DNA}) + 0.5 \epsilon(\text{PNA})$  is a constant for the same duplex.)

There is a random uncertainty in the optical density measurements that was determined from several UVM scans of the sample and estimated systematic uncertainties of  $0.002 \Delta G_b^\circ$  (UVM) from uncertainty in the concentration of the sample, of  $0.003 \Delta G_b^\circ$  (UVM) and  $0.003 \Delta H_v^\circ$  from uncertainty in the temperature of the sample, and of  $0.001 \Delta H_v^\circ$  from uncertainty

**Table 3.** Thermodynamic quantities for DNA/DNA and PNA/DNA hybridization reactions from ITC measurements

Duplex	Temperature (K)	<i>N</i>	<i>K</i> <sub>b</sub> (×10 <sup>6</sup> M <sup>-1</sup> )	-Δ <i>G</i> <sub>b</sub> <sup>°</sup> (kJ mol <sup>-1</sup> )	-Δ <i>H</i> <sub>b</sub> <sup>°</sup> (kJ mol <sup>-1</sup> )	- <i>T</i> Δ <i>S</i> <sub>b</sub> <sup>°</sup> (kJ mol <sup>-1</sup> )
DNA(TT)/DNA	296.7	1.02 ± 0.06	0.37 ± 0.07	31.6 ± 0.5	124 ± 12	92 ± 13
PNA(TT)/DNA	296.7	0.90 ± 0.05	1.8 ± 0.4	35.5 ± 0.5	93 ± 4	57 ± 4
DNA(TA)/DNA	296.4	0.91 ± 0.02	0.6 ± 0.2	32.7 ± 0.6	166 ± 8	133 ± 8
PNA(TA)/DNA	296.6	0.98 ± 0.08	5.8 ± 1.0	38.4 ± 0.4	140 ± 16	101 ± 16
DNA(TG)/DNA	296.9	0.99 ± 0.04	3.8 ± 0.5	37.4 ± 0.5	178 ± 8	141 ± 8
PNA(TG)/DNA	296.9	1.01 ± 0.06	7.7 ± 0.6	39.1 ± 0.2	141 ± 6	102 ± 6
DNA(TC)/DNA	296.7	0.97 ± 0.09	5.9 ± 1.6	38.4 ± 0.7	176 ± 17	138 ± 17
PNA(TC)/DNA	297.0	0.89 ± 0.01	3.1 ± 0.8	36.9 ± 0.6	112 ± 7	75 ± 7
DNA(AA)/DNA	298.1	0.84 ± 0.02	2.1 ± 1.2	36.1 ± 1.4	204 ± 8	168 ± 8
PNA(AA)/DNA	296.3	0.91 ± 0.03	13.5 ± 1.5	40.8 ± 0.3	102 ± 6	61 ± 6
DNA(AG)/DNA	296.4	1.04 ± 0.09	11.7 ± 1.3	40.1 ± 0.3	133 ± 6	93 ± 6
PNA(AG)/DNA	296.0	0.89 ± 0.03	28.3 ± 4.8	42.2 ± 0.4	89 ± 9	47 ± 10
DNA(AC)/DNA	296.5	0.95 ± 0.06	17.5 ± 2.5	41.1 ± 0.4	176 ± 5	135 ± 5
PNA(AC)/DNA	297.1	0.77 ± 0.06	8.3 ± 0.4	39.4 ± 0.1	122 ± 14	83 ± 14
PNA(GA)/DNA	296.1	0.97 ± 0.01	41.5 ± 7.5	43.2 ± 0.4	124 ± 11	81 ± 11
DNA(GG)/DNA	296.6	0.78 ± 0.08	1.2 ± 0.3	34.5 ± 0.7	178 ± 11	143 ± 11
PNA(GG)/DNA	298.0	0.97 ± 0.01	13.0 ± 4.0	40.6 ± 0.8	89 ± 4	48 ± 4
DNA(GT)/DNA	296.0	0.97 ± 0.01	0.29 ± 0.09	30.9 ± 0.8	157 ± 9	126 ± 9
PNA(GT)/DNA	297.1	1.06 ± 0.09	7.7 ± 1.2	39.2 ± 0.4	77 ± 7	38 ± 7
DNA(CC)/DNA	296.0	1.06 ± 0.02	18.8 ± 9.6	41.2 ± 1.3	179 ± 8	138 ± 8
PNA(CC)/DNA	296.4	0.98 ± 0.09	8.5 ± 0.4	39.3 ± 0.2	150 ± 24	111 ± 24
DNA(CT)/DNA	296.3	1.09 ± 0.03	4.5 ± 1.2	37.3 ± 0.7	174 ± 11	137 ± 11
PNA(CT)/DNA	295.8	1.06 ± 0.06	13.0 ± 2.0	40.3 ± 0.4	118 ± 5	78 ± 5
DNA(CG)/DNA	296.0	0.96 ± 0.03	14.5 ± 1.5	40.6 ± 0.3	223 ± 7	182 ± 7
PNA(CG)/DNA	295.9	0.97 ± 0.03	4.2 ± 0.2	37.5 ± 0.9	194 ± 24	156 ± 24
DNA(CA)/DNA	296.5	1.01 ± 0.03	10.3 ± 1.7	39.8 ± 0.9	203 ± 14	163 ± 14
PNA(CA)/DNA	295.8	0.98 ± 0.01	5.0 ± 0.4	37.9 ± 0.2	128 ± 12	90 ± 12

The standard uncertainties were determined from imprecision in the runs and systematic errors.

in the optical density reading. The random and estimated systematic uncertainties were combined in a quadrature to yield a combined standard uncertainty in the values for Δ*H*<sub>v</sub><sup>°</sup> and Δ*G*<sub>b</sub><sup>°</sup> (UVM).

## RESULTS

### ITC measurements

Results of a typical ITC run on the binding of DNA'(TG) to its complementary DNA sequence at 297.0 K are shown in Figure 1 along with its binding isotherm. Similar results were obtained from the ITC titration of DNA'(TG) into its complementary PNA sequence at 296.9 K, as shown in Figure 2. Average thermodynamic quantities for duplex formation resulting from least squares fits of the single site binding model (equation 2) to the binding isotherms are presented in Table 3 along with their corresponding Δ*G*<sub>b</sub><sup>°</sup> and *T*Δ*S*<sub>b</sub><sup>°</sup> values. Each entry in Table 3 is the average of the results from two or more different ITC runs at different PNA and DNA concentrations in the sample cell and in the syringe. The PNA solution was always in the sample cell because of its lower solubility relative to that of the complementary DNA. The stoichiometries of the binding reactions are also presented in Table 3 and are close to 1.0 with the exception of the DNA(GG)/DNA, DNA(AA)/DNA(TT), PNA(AC)/DNA, and PNA(TC)/DNA binding reactions. It is not clear as to why the DNA/DNA binding reactions exhibit low stoichiometries from 0.78 ± 0.08

to 0.84 ± 0.02. The low stoichiometries of the PNA binding reactions could be due to incorrect extinction coefficients for the two PNA sequences since the stoichiometries of the corresponding DNA/DNA binding reactions are close to 1.0. The ITC binding parameters did not exhibit any dependence on concentration of the DNA or PNA, although the concentration was changed by a factor of 2–3. Although the purity of the PNA(CC) sequence is considerably lower (85.6%) than the other PNA sequences, its DNA binding thermodynamic quantities are in the tables for comparison only. For the DNA/DNA binding reactions, the binding constants range from 0.29 × 10<sup>6</sup> M<sup>-1</sup> (Δ*G*<sub>b</sub><sup>°</sup> = -30.9 ± 0.8 kJ mol<sup>-1</sup>) for DNA(GT)/DNA to 1.9 × 10<sup>7</sup> M<sup>-1</sup> (Δ*G*<sub>b</sub><sup>°</sup> = -41.2 ± 1.3 kJ mol<sup>-1</sup>) for DNA(CC)/DNA, while the binding enthalpies range from -223 ± 7 kJ mol<sup>-1</sup> for DNA(CG)/DNA to -124 ± 12 kJ mol<sup>-1</sup> for DNA(TT)/DNA. Although the total range of 11 ± 2 kJ mol<sup>-1</sup> in the binding affinities (Δ*G*<sub>b</sub><sup>°</sup>) appears to be large with two base pair changes in the 10 base pair sequence, it is reasonable since Breslauer *et al.* (27) observed a change of 6.7 kJ mol<sup>-1</sup> in Δ*G*<sub>b</sub><sup>°</sup> between 5'-CAAATAAAG-3'/3'-GTTTATTTC-5' and 5'-CAAACAAAG-3'/3'-GTTTGTTC-5', where only one base pair is changed. However, in going from the DNA duplex 5'-CAAATAAAG-3'/5'-GTTTATTTC-3' to 5'-CAAAAAAAG-3'/3'-GTTTTTTTC-5', an enthalpy change of only 39 kJ mol<sup>-1</sup> was observed for the one base pair change (27) compared to 90 ± 9 kJ mol<sup>-1</sup> observed in this investigation. For the corresponding PNA/DNA binding reactions, the binding

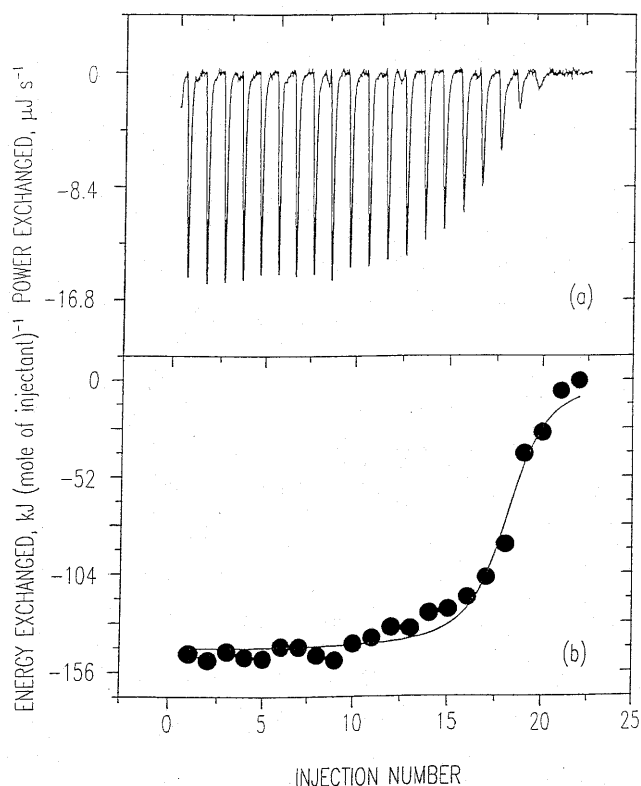


**Figure 2.** (a) The ITC scan consisting of the addition of 5  $\mu\text{l}$  aliquots of 0.801 mM DNA'(CA) to its complementary PNA(TG) sequence (0.051 mM) in PBS buffer at 296.9 K. (b) The binding isotherm for this titration.

constants range from  $1.8 \times 10^6 \text{ M}^{-1}$  ( $\Delta G_b^\circ = -35.5 \pm 0.5 \text{ kJ mol}^{-1}$ ) for PNA(TT)/DNA to  $4.15 \times 10^7 \text{ M}^{-1}$  ( $\Delta G_b^\circ = -43.2 \pm 0.4 \text{ kJ mol}^{-1}$ ) for PNA(GA)/DNA, while the binding enthalpies range from  $-194 \pm 24 \text{ kJ mol}^{-1}$  for PNA(CG)/DNA to  $-77 \pm 7 \text{ kJ mol}^{-1}$  for PNA(GT)/DNA. The binding affinities for the PNA/DNA sequences cover a higher range of values, thus indicating that the PNAs bind with a stronger affinity to their complementary DNA sequences than do the DNAs. This is not always true since comparison of the binding constants in Table 3 shows that the PNA binding constants are higher for eight of the 13 binding reactions and lower for five of the hybridization reactions. As seen in Table 3, this higher binding affinity results not so much from a more negative binding enthalpy but from a relatively smaller change in the binding entropy

### UVM measurements

Graphical results of typical UVM measurements on a DNA(TG)/DNA duplex at 5.2  $\mu\text{M}$  total strand concentration and on a PNA(TG)/DNA duplex at 6.2  $\mu\text{M}$  total strand concentration are presented in Figure 3. Although the PNA/DNA duplex melts at a higher temperature than does the DNA/DNA duplex, both duplexes have approximately the same binding affinities ( $-\Delta G_b^\circ$ ) at 297 K in Table 3. Average results from two or more of the optical density versus temperature scans for each duplex are summarized in Table 4. The transition temperatures range from 302.4 to 328.0 K for melting of the DNA/DNA duplexes and from 311.1 to 339.6 K for melting of the PNA/DNA duplexes. The DNA(TT)/DNA, DNA(TA)/DNA, and DNA(AA)/DNA duplex UVM curves were also scanned

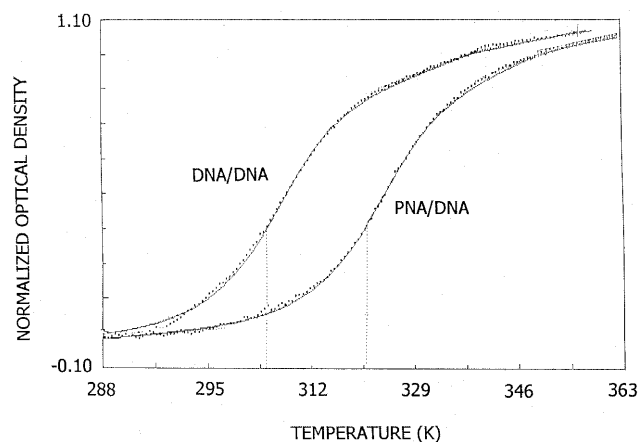


**Figure 3.** UVM measurements on a 0.0026 mM DNA(TG)/DNA duplex ( $C_t = 0.0052 \text{ mM}$ ) and on the PNA(TG)/DNA duplex ( $C_t = 0.0060 \text{ mM}$ ) in PBS solution. The vertical broken lines indicate the transition temperatures and the solid lines are least squares fits of the data to a two-state transition model.

from 287 to 363 K and it was found that the low temperature van't Hoff enthalpies and transition temperatures of these duplexes were the same as those determined from UVM curves scanned from 293 to 363 K. The van't Hoff enthalpies for dissociation of the duplex range from 165 [DNA(GG)/DNA] to 267  $\text{kJ mol}^{-1}$  [DNA(CC)/DNA] for melting of the DNA/DNA duplexes and from 170 [PNA(TT)/DNA] to 246 [PNA(CA)/DNA]  $\text{kJ mol}^{-1}$  for melting of the PNA/DNA duplexes. Results are not presented for the DNA(GT) duplexes since the transition temperature appeared too high to obtain a reasonable post-transitional baseline necessary for analysis of the data. For seven of the 12 DNA duplexes investigated, the absolute magnitude of the van't Hoff enthalpies are within two standard uncertainties of their corresponding ITC binding enthalpies. The exceptions are DNA(TT)/DNA, DNA(TA)/DNA, DNA(AG)/DNA, DNA(AC)/DNA, and DNA(CC)/DNA. The values of  $\Delta G_b^\circ$  (UVM), extrapolated to ambient temperature are within 8  $\text{kJ mol}^{-1}$  of their values determined by ITC for 10 of the 12 DNA duplexes. The discrepancies in the extrapolated  $\Delta G_b^\circ$  values may be due to incorrect determination of the van't Hoff enthalpy, the  $T_m$ , and the concentration in equation 6. Considering the range of the extinction coefficients for all the sequences is only from 0.9 to  $1.1 \times 10^5 \text{ l mol}^{-1} \text{ cm}^{-1}$  and the error in  $T_m$  is at most 2 K (<1%), the largest source of error would result from the van't Hoff enthalpy determination. Since the largest discrepancies between the  $\Delta G_b^\circ$  values are with DNA(AC)/DNA and DNA(CC)/DNA and to a lesser extent with DNA(TG)/DNA and DNA(TC)/DNA, their van't Hoff enthalpies were also determined by  $1/T_m$  versus  $\ln\{\text{OD}\}$  plots and are given in parentheses in Table 4. These values are within experimental error of those determined directly from UVM analysis of the single melting curves and, thus, the discrepancies cannot be attributed to incorrect determinations of the van't Hoff enthalpies. However, for melting of the PNA/DNA duplexes, the magnitudes of the van't Hoff enthalpies were almost twice the magnitudes of the ITC binding enthalpies and the discrepancies between the  $\Delta G_b^\circ$  values determined from the UVM and ITC measurements are much larger, up to 23  $\text{kJ mol}^{-1}$  for PNA(AG)/DNA. Since the largest

**Table 4.** Thermodynamic quantities from UVM measurements of the DNA/DNA and PNA/DNA duplexes

Duplex	$T_m$ (K)	$\Delta H_v$ (kJ mol <sup>-1</sup> ) <sup>a</sup>	$-\Delta H_b^\circ$ (ITC) (kJ mol <sup>-1</sup> )	$-\Delta G_b^\circ$ (UV) (kJ mol <sup>-1</sup> ) <sup>b</sup>	$-\Delta G_b^\circ$ (ITC) (kJ mol <sup>-1</sup> )
DNA(TT)/DNA	305.9–306.2	191 ± 8	124 ± 12	39 ± 1	31.6 ± 0.5
PNA(TT)/DNA	312.6	170 ± 10	93 ± 4	42.8 ± 0.5	35.5 ± 0.5
DNA(TA)/DNA	302.4–305.4	224 ± 11	166 ± 8	39.0 ± 0.3	32.7 ± 0.6
PNA(TA)/DNA	317.9–319.0	204 ± 27	140 ± 16	48 ± 2	38.4 ± 0.4
DNA(TG)/DNA	307.2–318.6	206 ± 11 (214 ± 24)	178 ± 8	46.0 ± 0.7	37.5 ± 0.5
PNA(TG)/DNA	317.8–330.3	223 ± 11 (217 ± 24)	141 ± 4	55 ± 1	39.1 ± 0.2
DNA(TC)/DNA	314.1	229 ± 10 (208 ± 10)	176 ± 16	45.9 ± 0.5	38.4 ± 0.7
PNA(TC)/DNA	320.5–324.2	226 ± 12 (225 ± 3)	112 ± 6	51.9 ± 0.5	36.9 ± 0.6
DNA(AA)/DNA	311.6–315.5	192 ± 4	204 ± 5	42.2 ± 0.2	36.1 ± 1.4
PNA(AA)/DNA	317.2–330.4	232 ± 12 (247 ± 7)	102 ± 3	56.3 ± 0.7	40.8 ± 0.3
DNA(AG)/DNA	318.3	187 ± 2	133 ± 6	46 ± 2	40.1 ± 0.3
PNA(AG)/DNA	330.4–338.6	310.2–320.6	89 ± 9	66.7 ± 0.8	42.2 ± 0.4
DNA(AC)/DNA	310.2–320.6	239 ± 12 (220 ± 24)	176 ± 1	50 ± 1	41.1 ± 0.4
PNA(AC)/DNA	322.3	221 ± 11	122 ± 14	51 ± 1	39.4 ± 0.1
PNA(GA)/DNA	312.0–339.6	275 ± 25 (232 ± 37)	124 ± 11	67 ± 3	43.2 ± 0.4
DNA(GG)/DNA	312.0–319.5	165 ± 9	178 ± 9	42 ± 1	34.5 ± 0.7
PNA(GG)/DNA	335.5–336.0	204 ± 10	89 ± 2	57 ± 1	40.6 ± 0.8
DNA(CC)/DNA	316.9–324.4	267 ± 27 (224 ± 31)	180 ± 4	56 ± 4	41.2 ± 1.3
PNA(CC)/DNA	333.6–335.9	254 ± 6	150 ± 24	51 ± 1	39.3 ± 0.2
DNA(CT)/DNA	315.0–317.1	205 ± 21	174 ± 9	40 ± 1	37.3 ± 0.7
PNA(CT)/DNA	324.1–329.7	242 ± 8	118 ± 1	47 ± 2	40.3 ± 0.4
DNA(CG)/DNA	326.3–328.0	245 ± 10	223 ± 3	46 ± 1	40.6 ± 0.3
PNA(CG)/DNA	311.1, 362.2	Two two-state transitions were observed			
DNA(CA)/DNA	319.4–319.8	200 ± 8	203 ± 14	41 ± 1	39.8 ± 0.9
PNA(CA)/DNA	333.2–334.6	246 ± 9	128 ± 12	49 ± 1	37.9 ± 0.2

<sup>a</sup>van't Hoff enthalpies in parentheses were determined from the slope of  $1/T_m$  versus  $\ln(\text{OD})$  plots.

<sup>b</sup> $\Delta G_b^\circ(\text{UV}) = -RT_m \ln(4C_1^{-1}) - \Delta H_v[1 - T(\text{ITC})/T_m]$  where ITC is the ITC measurement temperature (Table 1).

discrepancies in the  $\Delta G_b^\circ$  values are with PNA(TG)/DNA, PNA(TC)/DNA, PNA(AA)/DNA, PNA(AG)/DNA, and PNA(GA)/DNA, their van't Hoff enthalpies were also determined by  $1/T_m$  versus  $\ln\{\text{OD}\}$  plots and are given in parentheses in Table 4. These values are again within experimental error of those determined directly from UVM analysis of the single melting curves.

## DISCUSSION

The ITC results yield direct determinations of the binding constant and binding enthalpy at ambient temperatures and, accordingly, would be more accurate than the extensively used UVM determinations, which rely on extrapolation of the high temperature changes down to ambient temperatures. The affinities for PNA binding to their complementary DNA sequences are in the order PNA(GA) = PNA(AG) > PNA(AA) = PNA(GG) = PNA(CT) > PNA(AC) = PNA(GT) = PNA(CC) = PNA(TG) > PNA(TA) = PNA(CA) = PNA(CG) > PNA(TC) > PNA(TT), where equality between two values means one value is within one standard deviation of the other. It appears that the highest PNA binding affinities occur with a large number of purine bases in the PNA sequence. More specific attempts to fit the binding affinities to a predictive scheme based on the PNA sequence, such as the nearest neighbor Watson–Crick pair method employed for DNA duplexes, were unsuccessful. The nearest neighbor Watson–Crick pair predictive scheme assigns  $\Delta G_b^\circ$ ,  $\Delta H_b^\circ$ , and  $\Delta S_b^\circ$  values to

each of the nearest neighbor Watson–Crick pairs identified in the DNA/DNA sequence and totals these contributions to predict a value for the total DNA/DNA binding reaction at 1.0 M salt concentration and pH 7.0 (27,28). In particular, as shown in Table 3, the range of  $\Delta G_b^\circ$  values for the different 10mer duplexes is <8 kJ mol<sup>-1</sup>, which is too limited a range of values to determine accurate  $\Delta G_b^\circ$  assignments for the different nearest neighbor pairs. It is necessary to obtain a wider range of values by going to shorter and longer sequences to determine accurate assignments.

The ITC results show that the DNA binding affinities follow a different dependence on sequence than do their corresponding PNA sequences. For DNA binding to its complementary DNA sequence, the binding affinities are DNA(CC) = DNA(AC) > DNA(CG) = DNA(AG) = DNA(CA) > DNA(TC) > DNA(TG) = DNA(CT) > DNA(AA) > DNA(GG) > DNA(TA) > DNA(TT) = DNA(GT). At 1 M salt concentration, the DNA/DNA binding affinities are predictable from the number and type of nearest neighbor Watson–Crick pairs (27,28). With the exception of the DNA'(CG), DNA'(TG), DNA'(GG), DNA'(GT), and DNA'(GA) sequences, the DNA sequences bind with greater affinities to their complementary PNA sequences than to their complementary DNA sequences. In addition, the PNA/DNA and DNA/DNA base pair sequences appear to exhibit the same amount of specificity in their binding affinities. The implied higher specificity of PNA sequences was observed in the thermodynamic quantities determined from the UVM measurements (5)

which have been shown to also depend on thermodynamic differences between the strand states at the melting temperature and at ambient temperature. The corresponding UVM results on the DNA/DNA duplexes extrapolate down to a consistently lower  $\Delta G_b^\circ$  by at least  $-8 \text{ kJ mol}^{-1}$  than those determined directly from the ITC measurements at ambient temperature. However, for seven out of the 12 DNA/DNA duplexes, the absolute magnitudes of the van't Hoff enthalpies are in agreement with the absolute magnitudes of the ITC binding enthalpies. This near agreement between the two methods is remarkable in the light of recent comparisons between ITC determined binding enthalpies and van't Hoff enthalpies which show differences of up to 50% between their values for protein–ligand, protein–peptide, and cyclodextrin–alcohol binding reactions (40).

The disparities between the extrapolated UVM results on the melting of the PNA/DNA duplexes and the ITC results on their formation at ambient temperature may result from several sources. The UVM results are based on applying a two-state transition model to the changes in the optical density upon rapid melting of the duplex. It will be shown in a subsequent paper (41) that differential scanning calorimetry measurements on melting of the PNA/DNA and DNA/DNA duplexes yield model-independent binding enthalpies in agreement with the UVM results in this investigation. Thus, the most likely source for this disparity between the UVM and ITC results on the duplexes is the thermodynamic differences between the DNA and PNA strand states at the melting and at ambient temperature which would make different, undetermined contributions to the thermodynamics of duplex formation. This was observed for a 13mer DNA/DNA duplex where the thermodynamic states of the single strands were already in a configuration conducive to duplex formation (32). Ratilainen *et al.* (31) also observed thermodynamic contributions from conformational changes of lysine-tagged single PNA strands binding to their complementary DNA sequences to form 10mer duplexes. Assuming that binding of the PNA or DNA strands to their complementary DNA strands at ambient temperature occurs, respectively, with

$$\Delta G_b^\circ (\text{ITC}) = \Delta G_m^\circ(\text{PNA}) + \Delta G_m^\circ(\text{DNA}) + \Delta G_b^\circ(\text{PNA/DNA}) \quad \mathbf{7a}$$

$$\Delta G_b^\circ (\text{ITC}) = \Delta G_m^\circ(\text{DNA}) + \Delta G_m^\circ(\text{DNA}) + \Delta G_b^\circ(\text{DNA/DNA}) \quad \mathbf{7b}$$

where  $\Delta G_b^\circ$  (ITC) is the observed ITC value,  $\Delta G_m^\circ(\text{PNA})$  and  $\Delta G_m^\circ(\text{DNA})$  are the free energy changes for converting, respectively, the PNA and DNA strand states at ambient temperature to the random coil states at the melting temperature, and  $\Delta G_b^\circ(\text{PNA/DNA})$  and  $\Delta G_b^\circ(\text{DNA/DNA})$  are the binding affinities between the random PNA and DNA strands. Then,

$$\Delta H_b^\circ (\text{ITC}) = \Delta H_m^\circ(\text{PNA}) + \Delta H_m^\circ(\text{DNA}) + \Delta H_b^\circ(\text{PNA/DNA}) \quad \mathbf{8a}$$

$$\Delta H_b^\circ (\text{ITC}) = \Delta H_m^\circ(\text{DNA}) + \Delta H_m^\circ(\text{DNA}) + \Delta H_b^\circ(\text{DNA/DNA}) \quad \mathbf{8b}$$

and

$$\Delta S_b^\circ (\text{ITC}) = \Delta S_m^\circ(\text{PNA}) + \Delta S_m^\circ(\text{DNA}) + \Delta S_b^\circ(\text{PNA/DNA}) \quad \mathbf{9a}$$

$$\Delta S_b^\circ (\text{ITC}) = \Delta S_m^\circ(\text{DNA}) + \Delta S_m^\circ(\text{DNA}) + \Delta S_b^\circ(\text{DNA/DNA}) \quad \mathbf{9b}$$

where, again, the (ITC) values are the observed ITC values,  $\Delta H_m^\circ(\text{PNA})$ ,  $\Delta H_m^\circ(\text{DNA})$ ,  $\Delta S_m^\circ(\text{PNA})$  and  $\Delta S_m^\circ(\text{DNA})$  are the enthalpy and entropy changes for converting the PNA and DNA strand states to the random coil states, and  $\Delta H_b^\circ(\text{PNA/DNA})$  and  $\Delta S_b^\circ(\text{PNA/DNA})$  are the enthalpy and entropy changes for PNA/DNA duplex formation from the random coil strands. Taking  $\Delta H_b^\circ(\text{PNA,DNA/DNA}) = -\Delta H_v$  determined from the UVM measurements then  $\Delta H_m^\circ(\text{PNA}) + \Delta H_m^\circ(\text{DNA}) > 0$  and  $\Delta H_m^\circ(\text{DNA}) + \Delta H_m^\circ(\text{DNA}) > 0$ . Since  $\Delta G_m^\circ(\text{PNA}) + \Delta G_m^\circ(\text{DNA}) > 0$  and  $\Delta G_m^\circ(\text{DNA}) + \Delta G_m^\circ(\text{DNA}) > 0$ , then  $\Delta S_m^\circ(\text{PNA}) + \Delta S_m^\circ(\text{DNA}) > 0$  and  $\Delta S_m^\circ(\text{DNA}) + \Delta S_m^\circ(\text{DNA}) > 0$ . The thermodynamic contributions of converting the ordered strands at ambient temperature to random coil states for formation of the PNA/DNA and DNA/DNA duplexes are endothermic and are driven by an increase in entropy. This reduces the exothermicity of the binding reaction at ambient temperature but also reduces the entropic cost of the binding reaction since the reactants are already in partially ordered strand states prior to the binding reaction. For formation of the DNA/DNA duplexes where  $\Delta G_b^\circ$  (ITC) –  $\Delta G_b^\circ(\text{DNA/DNA})$  are within  $8 \text{ kJ mol}^{-1}$  and seven of 12 binding enthalpies agree with the UVM van't Hoff enthalpies, i.e.  $\Delta H_m^\circ(\text{DNA}) + \Delta H_m^\circ(\text{DNA}) = \Delta H_v$ , these thermodynamic contributions are less than for formation of the PNA/DNA duplexes where these differences are larger (7–24 and 60–170  $\text{kJ mol}^{-1}$ , respectively). Since the entropy cost is even less for the PNA/DNA duplexes than for the corresponding DNA/DNA duplexes (Table 1), then the PNA strand is more ordered than the corresponding DNA strand. Perhaps the PNA strands tend to 'stack' the nucleotide bases, which would be enhanced by the greater flexibility of the peptide backbone than the DNA strands. Furthermore, Tomac *et al.* (30) have reported two-state-like melting transitions of two single-stranded 10 base PNAs around 317 K but with van't Hoff enthalpies of melting much higher ( $\sim 276 \text{ kJ mol}^{-1}$ ). The stacking of the PNA sequences may affect the value of the extinction coefficient of the PNA used in determination of the PNA concentration at ambient temperatures, but this effect seems to be small since the stoichiometry of the PNA/DNA hybridization reactions is close to 1.0 (actually  $0.95 \pm 0.06$ ). More importantly, the ordered configurations for the PNA strands and for half the DNA strands at ambient temperature must be taken into consideration when using melting temperatures to compare the duplex binding affinities at ambient temperature.

## ACKNOWLEDGEMENTS

This work was supported by NIST ATP grant ATP99 to F.P.S. Certain commercial equipment, instruments, and materials are identified in this paper in order to specify the experimental procedure as completely as possible. In no case does this identification imply a recommendation or endorsement by the National Institute of Standards and Technology, nor does it imply that the material, instrument, or equipment identified is necessarily the best available for the purpose.

## REFERENCES

- Nielson, P.E., Engholm, M., Berg, R.H. and Burchardt, O. (1991) *Science*, **254**, 1497–1500.

2. Egholm, M., Burchardt, O., Nielsen, P.E. and Berg, R.H. (1992) *J. Am. Chem. Soc.*, **114**, 1895–1897.
3. Harvey, J.C., Peffer, N.J., Bisi, J.E., Thomson, S.A., Cadilla, R., Josey, J.A., Ricca, D.J., Hassman, C.F., Bonham, M.A., Au, K.G., Carter, S.G., Brukstein, D.A., Boyd, A.L., Noble, S.A. and Babiss, L.E. (1992) *Science*, **258**, 1481–1485.
4. Buchardt, O., Egholm, M., Berg, R.H. and Nielsen, P.E. (1993) *Trends Biotechnol.*, **11**, 384–386.
5. Egholm, M., Buchardt, O., Christensen, L., Behrens, C., Freier, S.M., Driver, D.A., Berg, R.H., Kim, S.K., Norden, B. and Nielsen, P.E. (1993) *Nature*, **365**, 566–568.
6. Brown, S.C., Thomson, S.A., Veal, J.M. and Davis, D.G. (1994) *Science*, **265**, 777.
7. Wittung, P., Nielsen, P.E., Burchardt, O., Egholm, M. and Norden, B. (1994) *Nature*, **368**, 561–563.
8. Demers, D.B., Curry, E.T., Egholm, M. and Sozer, A.C. (1995) *Nucleic Acids Res.*, **23**, 3050–3055.
9. Orum, H., Koch, T., Egholm, M., O'Keefe and Coull, J. (1997) In Taylor, G.R. (ed.), *Laboratory Methods for the Detection of Mutations and Polymorphisms in DNA*. CRC Press, Boca Raton, FL, Ch. 11, pp. 123–133.
10. Orum, H., Nielsen, P.E., Jorgensen, M., Larsson, C., Stanley, C. and Koch, T. (1995) *Biotechniques*, **19**, 472–480.
11. Boffa, L.C., Carpaneto, E.M. and Allfrey, V.G. (1995) *Proc. Natl Acad. Sci. USA*, **92**, 1901–1905.
12. Orum, H., Nielsen, P.E., Egholm, M., Berg, R.H., Buchardt, O. and Stanley, C. (1993) *Nucleic Acids Res.*, **21**, 5332–5336.
13. Thiede, C., Bayerdorffer, E., Blasczyk, R., Wittig, B. and Neubauer, A. (1996) *Nucleic Acids Res.*, **24**, 983–984.
14. Norton, J.C., Piatyszek, M.A., Wright, W.E., Shay, J.W. and Corey, D.R. (1996) *Nature Biotechnol.*, **14**, 615–619.
15. Nielsen, P.E., Egholm, M. and Buchardt, O. (1994) *Gene*, **149**, 139–145.
16. Hirschman, S.Z. and Chen, C.W. (1996) *J. Invest. Med.*, **44**, 347–351.
17. Wang, J., Palecek, E., Nielsen, P.E., Rivas, G., Cai, X.H., Shiraishi, H., Dontha, N., Luo, D.B. and Farias, P.A.M. (1996) *J. Am. Chem. Soc.*, **118**, 7667–7670.
18. Kim, S.K., Nielsen, P.E., Egholm, M., Buchardt, O., Kristensen, S.M. and Ericksson, M. (1993) *Biochemistry*, **115**, 6477.
19. Leijon, M., Graslund, A., Nielsen, P.E., Buchardt, O., Norden, B., Kristensen, S.M. and Erikson, M. (1994) *Biochemistry*, **33**, 9820–9825.
20. Kastrup, J.S., Pilgaard, M., Jorgensen, F.S., Nielsen, P.E. and Rasmussen, H. (1995) *FEBS Lett.*, **363**, 115–117.
21. Betts, L., Josey, J.A., Veal, J.M. and Jordan, S.R. (1995) *Science*, **270**, 1838–1841.
22. Rasmussen, H., Kastrup, J.S., Nielsen, J.N., Nielsen, J.M. and Nielsen, P.E. (1997) *Nature Struct. Biol.*, **4**, 98–101.
23. Takao, T., Fukuda, H., Coull, J. and Shimonishi, Y. (1994) *Rapid Commun. Mass Spectrom.*, **8**, 925–928.
24. Griffith, M.C., Risen, L.M., Greig, M.J., Lesnik, E.A., Sprankle, K.G., Griffey, R.H., Kiely, J.S. and Freier, S.M. (1995) *J. Am. Chem. Soc.*, **117**, 831–832.
25. Butler, J.M., Jiang-Baucom, P., Huang, M., Belgrader, P. and Girard, J. (1996) *Anal. Chem.*, **68**, 3283–3287.
26. Hyndman, D., Cooper, A., Pruzinsky, S., Coad, D. and Mitsuhashi, M. (1996) *Biotechniques*, **20**, 1090–1092.
27. Breslauer, K.J., Frank, R., Blocker, H. and Marky, L.A. (1986) *Proc. Natl Acad. Sci. USA*, **83**, 3746–3750.
28. Santa Lucia, J., Allawi, H.T. and Seneviratne, P.A. (1996) *Biochemistry*, **35**, 3555–3562.
29. Giesen, U., Kleider, W., Berding, C., Geiger, A., Orum, H. and Nielsen, P.E. (1998) *Nucleic Acids Res.*, **26**, 5004–5006.
30. Tomac, S., Sarkar, M., Ratilainen, T., Wittung, P., Nielsen, P.F., Norden, B. and Graslund, A. (1996) *J. Am. Chem. Soc.*, **118**, 5544–5552.
31. Ratilainen, T., Holmen, A., Tuite, E., Haaima, G., Christensen, L., Nielsen, P.E. and Norden, B. (1998) *Biochemistry*, **37**, 12331–12342.
32. Vesnaver, G. and Breslauer, K.J. (1991) *Proc. Natl Acad. Sci. USA*, **88**, 3569–3573.
33. Kallansrud, G. and Ward, B. (1996) *Anal. Biochem.*, **236**, 134–138.
34. Cantor, C.R., Warshaw, M.M. and Shapiro, H. (1970) *Biopolymers*, **9**, 1059–1077.
35. Wiseman, T., Williston, S., Brandts, J.F. and Lin, L.N. (1989) *Anal. Biochem.*, **179**, 131–137.
36. Schwarz, F.P., Puri, K., Bhat, R.G. and Suroliya, A. (1993) *J. Biol. Chem.*, **268**, 7668–7677.
37. Kirchoff, W.H. (1993) *Exam: A Two-State Thermodynamic Analysis Program*, NIST Technical Note 1401. NIST, US Government Printing Office, Washington, DC.
38. Marky, L.A. and Breslauer, K.J. (1987) *Biopolymers*, **26**, 1601–1620.
39. Borer, P.N., Dengler, B. and Tinoco, I. (1974) *J. Mol. Biol.*, **86**, 843–853.
40. Naghibi, H., Tamura, A. and Sturtevant, J.M. (1995) *Proc. Natl Acad. Sci. USA*, **92**, 5597–5599.
41. Chakrabarti, M.C. and Schwarz, F.P. (1999) *Nucleic Acids Res.*, **27**, 4801–4806.